JOURNAL OF Applied Polymer SCIENCE

Synthesis and Characterization of Molybdenum-Modified Polycarbosilane for SiC(Mo) Ceramics

Zhengfang Xie, Jiaxin Niu, Zhaohui Chen
National Key Laboratory of Science and Technology on Advanced Ceramic Fibres and Composites, College of Aerospace Science & Engineering, National University of Defense Technology, Changsha 410073, China
Correspondence to: Z. Xie (E-mail: xiezhengfang@163.com)

ABSTRACT: A novel molybdenum-containing polycarbosilane, polymolybdenocarbosilane (PMoCS), for SiC(Mo) fiber has been synthesized from polysilacarbosilane (PSCS) and $MoCl_5$ as raw materials. The synthesis conditions is investigated. Characterization performed on the as-synthesized PMoCS includes Fourier Transformed Infrared Spectroscopy (FT IR), gel-permeation chromatography (GPC), X-ray photoelectron spectroscopy (XPS), ^1H NMR, and ^{29}Si NMR, respectively. The polymer-to-ceramic conversion is studied with thermogravimetric analysis (TGA) and X-ray diffraction (XRD). Preliminary research on the melt spinnability of PMoCS is carried out. The results show that the synthesis reaction is temperature-dependent. Mo exists mainly as Si—Mo bonds. The reaction mechanism is believed to involve HCl elimination between Si—H and Mo—Cl, and followed by the Kumada rearrangement. The ceramic yield of PMoCS, prepared with 10 wt % $MoCl_5$, is approximately 78.5% at 1200°C in a N_2 flow. The XRD results suggest that ceramics pyrolyzed in the range of 800–1000°C are all amorphous, while β-SiC and β-$MoSi_2$ crystals are observed at 1200 and 1400°C, respectively. The conversion from β-$MoSi_2$ to α-$MoSi_2$ is almost completed at 1600°C. PMoCS is melt spinnable into flexible and uniform green fibers with the diameters about 13.4 μm to 12.2 μm. © 2012 Wiley Periodicals, Inc. J. Appl. Polym. Sci. 000: 000–000, 2012

KEYWORDS: polymolybdenocarbosilane; synthesis; characterization; reaction mechanism; pyrolysis

Received 4 January 2012; accepted 12 July 2012; published online
DOI: 10.1002/app.38344

INTRODUCTION

The polymer-derived ceramic technique is a chemical process in which preceramic polymers are thermally decomposed in a controlled atmosphere into nonoxide covalently bonded ceramics.[1–3] Many preceramic polymers have been developed in the last three decades. In paticularly, Si-based polymers, such as polycarbosilanes (PCS), polysilazanes, polysiloxanes, polycarbosilazanes, and boron-modified polysilazanes or polyborosilazanes have proven to be promising precursors.[1–11] The significant advantage of the technique is the chemistry (elemental composition, compositional homogeneity and atomic architecture) and the shaping properties of preceramic polymers to be controlled and designed in order to produce ceramics with desirable composition, structure with shapes from 0D to 3D morphologies, such as fibers, coatings, mesoporous, monoliths, or complex shaped parts.[12–17] Especially, the technique provides an extremely important approach to the ceramic fiber fabrication, particularly for the SiC fibers with diameters of 10–15 μm.[18–33] Continuous SiC fibers serve as high-temperature materials in many fields. High-temperature performance requirements, meanwhile, become more and more rigorous along with the development of high-temperature materials such as ceramic matrix composites for advanced energy and propulsion applications.[1–10]

Three generations of polymer-derived SiC fibers have been developed by COI Ceramics, from Nicalon® (1st generation) and Hi-Nicalon-S® (2nd generation) to Sylramic™ (3rd generation).[1–10,18–23] Restricted by the decomposition of Si—O—C and β-SiC grain growth, Nicalon® can be used at up to 1200°C under inert atmosphere and about 1000°C in air. The research showed that, the thermal stability of SiC fiber depends on the composition and microstructures of SiC fiber. Above 1200°C, the release of gaseous species CO and/or SiO as well as the grain growth and coarsening lead to the breakdown of fibers and the loss of shape integrity. To increase the thermal stability of SiC fiber, amorphous state as well as the decrease of oxygen content are required. To decrease its oxygen content, an irradiation crosslinking technique has been adopted. Hi-Nicalon-S®, on the other hand, is a near-stoichiometric SiC fiber with a heat-resistance temperature of 1600°C under inert atmosphere, and strength retention of 60% after exposure to air at 1400°C for 10 h. Heteroelements, such as

Ti, Zr, B, Al, are introduced as sintering aids and grain growth inhibitors in this 2nd generation SiC fiber. Sylramic™, exhibits 200°C higher heat-resistance under inert atmosphere than its previous generation, and strength retention of 66% after exposure to air at 1370°C for 12 h. Creep and strength retention close to those of bulk SiC are found in Sylramic™ at high temperatures.[1,2,11–33]

$MoSi_2$, very oxidation resistant, has a melting point of 2020°C and shows a decent plastic deformation capacity. SiC-$MoSi_2$ composites are therefore used as high-temperature structural materials and heating elements, owing to their excellent high-temperature resistance, oxidation resistance, high creep resistance, high heat conductivity, and high electrical conductivity.[34]

A molybdenum-containing preceramic polymer, MoPMS, was reportedly synthesized through HCl elimination between polymethylsilane and $MoCl_5$ in tetrahydrofuran. SiC–$MoSi_2$ ceramics were obtained after pyrolzed at 1400°C in an argon atmosphere with a yield about 88%. Besides β-SiC grain, Mo-Si phases such as $MoSi_2$ and Mo_5Si_3 were also produced.[35] However, the as-synthesized MoPMS is insoluble or infusible, suggesting it is rather difficult to spin fibers and prepare SiC–$MoSi_2$ fibers from this polymer, which is evidenced by the fact that few reports on the SiC–$MoSi_2$ fibers are found.

Following the strategy of introducing heteroelements at an atomic scale, a novel precursor of molybdenum-modified PCS, polymolybdenocarbosilane (PMoCS), for SiC(Mo) ceramic fibers is synthesized and characterized in this work. The obtained Si-based ceramic fibers are expected to exhibit good high-temperature resistance and excellent oxidation resistance, and therefore, to increase the lifetime of SiC fibers. To reduce the oxygen content and improve the reactivity, $MoCl_5$ is employed as the Mo source reagent.

Molybdenum-containing polycarbosilane, PMoCS has been synthesized and characterized by means of Fourier Transformed Infrared Spectroscopy (FT IR), gel-permeation chromatography (GPC), X-ray photoelectron spectroscopy (XPS), ^{1}H NMR, and ^{29}Si NMR, respectively. Preliminary study of the melt spinnability of the as-synthesized polymer was also carried out. The ceramic conversion was researched. The as-synthesized polymers were subsequently pyrolyzed ranged from 800°C to 1600°C in a nitrogen atmosphere.

EXPERIMENTAL

General Procedures

Material. $MoCl_5$ was purchased from J & K Chemical (China). polydimethylsilane (PDMS, $-[Si(CH_3)_2]_n-$) was purchased from Shenzhen Gujia chemical, China. Polysilacarbosilane (PSCS), a viscous polymer with a basic structure of $-(MeHSiCH_2)_x-(SiMe_2)_{(1-x)}-$, was obtained from the thermolysis of PDMS at 400°C in a N_2 flow.

Synthesis of PMoCSs. PMoCS was synthesized from the reaction of PSCS with $MoCl_5$ in an argon atmosphere, using argon/vacuum lines and Schlenk-type flasks.

First, $MoCl_5$ was introduced in a three-necked flask in a glove-box. PSCS was then introduced to the flask at room temperature. It was then heated up to the prerequisite temperature for a few hours in an argon flow. After cooling to room temperature, the polymer was purified through dissolving in xylene and followed by solution filtration. The filtrate was concentrated in high vacuum (10^{-2} mbar) at room temperature to remove all solvents and give an air- and moisture-stable black-colored solid polymer of PMoCS.

Polymer Green Fiber Preparation. Preliminary study of the melt spinnability of the as-synthesized polymer was also carried out. Polymer green fibers were prepared by a lab-scale melt-spinning apparatus. PMoCS was molten by heating within a heater block until an appropriate viscosity was obtained. The molten polymer flowing was then driven through a filter and spinneret having a single 200 nm capillary under a certain pressure. The as-extruded molten filament was stretched and continuously collected on a rotating spool.

Characterization

The as-synthesized polymers were characterized with many spectroscopic techniques. FTIR spectroscopy was measured over a range of 4000 to 400 cm^{-1} in KBr pellets on a Nexus 670 FTIR spectrophotometer. ^{1}H and ^{29}Si NMR spectra were recorded on a Bruker DMX 600 spectrometer with tetramethylsilane as a chemical shift reference and $CDCl_3$ as a solvent. XPS was carried out on an ESCALAB MK II of VG Scientific Ltd. The molecular weight distributions of PMoCSs were characterized by a GPC instrument (Waters-1515), where tetrahydrofuran (THF) was used as a solvent at a flow rate of 1 mL min^{-1} with polystyrene as a standard specimen. The melting point (m.p.) of the polymers was measured with a WRS-2A/2 melting point apparatus made by Shanghai Jinmi Co. (China). Polymer samples were crushed into powders

Table I. Influence of the Reaction Temperature on the Yield, Molecular Weight, and Melting Point (m.p.) of the As-Synthesized Polymers

Polymers	Reaction temperature (°C)	Yield (%)	m.p. (°C)	$\overline{Mn}^a$	$\overline{Mw}^b$	Polydispersity index
PMoCS-420	420	56.1	85	1368	5046	3.69
PMoCS-430	430	56.6	125	1422	6209	4.37
PMoCS-440	440	58.9	150	1656	7081	4.28
PMoCS-450	450	59.5	220	1926	17613	9.14
PMoCS-460	460	-[c]	300	2610	46157	17.68

[a]Number average molecular weight according to the GPC results, [b]weight average molecular weight according to the GPC results, [c]Partially crosslinked.

and charged into a capillary before melting point measurement. The temperature corresponding to the first bright spot was regarded as the melting point of the polymer. Three specimens were tested for each sample and the values were then averaged to obtain a melting temperature. Thermogravimetric analysis (TGA) was carried out using a NETZSCH STA 449C instrument with a heating rate of 10°C min^{-1} up to 1200°C in a nitrogen flow at 40 mL min^{-1}. The chemical compositions of the derived ceramics were measured for Si, C, and O. X-ray diffraction (XRD) patterns of the derived ceramics were obtained on a Siemens D-500 diffractometer (Germany) using Cu *Kα* radiation.

Chemical composition of derived ceramics were measured. Si content was determined with an optical emission spectrometer ARL 3580 B (ARL, EcuBlens, Switzerland). The quantitative analyzes of oxygen and carbon were obtained by using a carrier gas heat extraction analyzer TC -436 (LECO) and C-200(LECO), respectively.

RESULTS AND DISCUSSION

Synthesis of PMoCS

Usually, the reaction temperature and stoichiometric ratio of reactants greatly affect the properties of the product polymer. In the current study, the influence of the reaction temperature on the characteristics of as-synthesized polymers was investigated. PSCS was reacted with 2 wt % $MoCl_5$ at different temperatures with a dwelling time of 10 h. The yield, molecular weight, and melting point (m.p.) of the polymers synthesized at different temperatures are summarized in Table I.

The as-synthesized polymers of PMoCS-420 (the number denotes the reaction temperature), PMoCS-430, PMoCS-440, and PMoCS-450, are dark-colored, fusible, and easily soluble in organic solvents such as cyclohexane, THF, and xylene, while PMoCS-460 exhibits an extra high melting point likely because it is partially crosslinked. The results suggest that the reaction is a temperature-dependent process. As shown in Figure 1, the molecular weight increases and the molecular weight distribution broadens as the reaction temperature increases. The molecular weight, melting point, and the polydispersity index ($\overline{Mw}/\overline{Mn}$) of the as-synthesized polymers increase quickly when the temperature is higher than

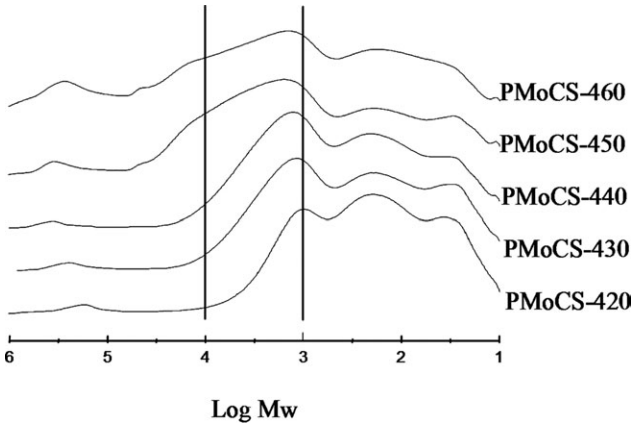

Figure 1. Molecular weight distributions of PMoCSs synthesized at different temperatures.

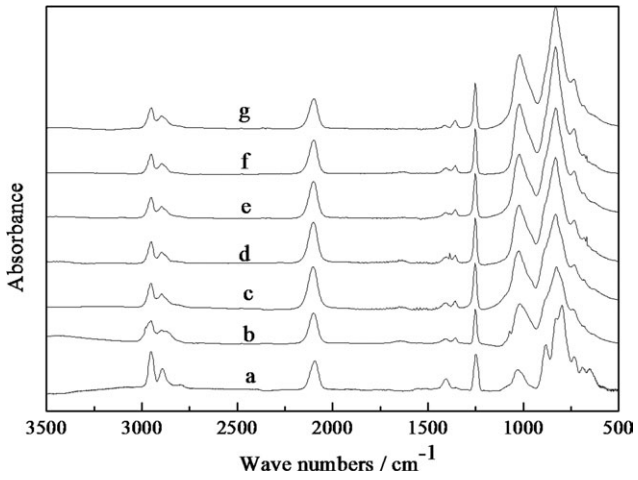

Figure 2. FTIR spectra of PMoCSs, PSCS, and PCS (a: PSCS, b: PCS, c: 2 wt %, d: 4 wt %, e: 6 wt %, f: 8 wt %, and g: 10 wt %).

450°C, with highest values observed in PMoCS-460, again because it is a partially crosslinked polymer. The molecular weight distributions of these polymers are plotted in Figure 1.

Characterization of PMoCSs

FTIR. The FTIR spectra of PMoCSs from different dosages of $MoCl_5$ are shown in Figure 2, along with those of PSCS and PCS for comparison purposes. The polymers exhibit common infrared bands at 2950 cm^{-1}(ν(C—H)), 2100 cm^{-1} (ν(Si—H)), 1410 cm^{-1} ($\nu(CH_3)$), 1357 cm^{-1}($\nu(CH_2)$ in Si—CH_2—Si moieties), and 1252 cm^{-1} (ν(Si—CH_3)). A broad band centered at 1060 cm^{-1} is assigned to the Si—O—Si units and CH_2 wagging in the Si—CH_2—Si moieties. Peaks at 690–860 cm^{-1} are attributed to Si—CH_3 wagging and Si—C stretching. Particularly, the presence of the CH_2 wagging vibration in the Si—CH_2—Si units indicates the formation of the PCS basal structure in PMoCS through the Kumada rearrangement. All the peaks are in good agreement with those of PCS reported in the literature.[7,8,31,36–38] Mo—Si bonds are not identified.

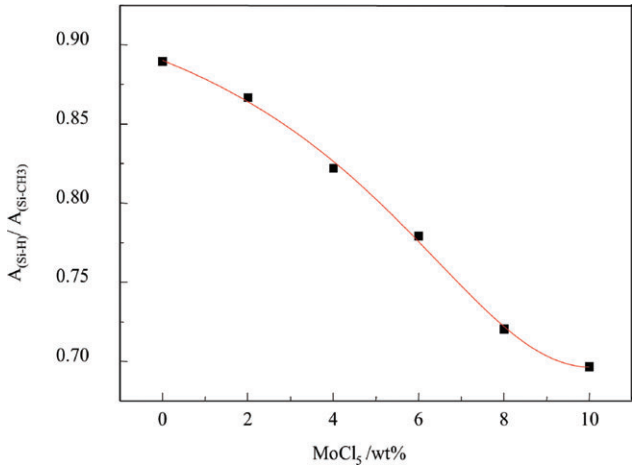

Figure 3. Absorbency ratio in the function of the dosages of $MoCl_5$. [Color figure can be viewed in the online issue, which is available at wileyonlinelibrary.com.]

Applied Polymer SCIENCE

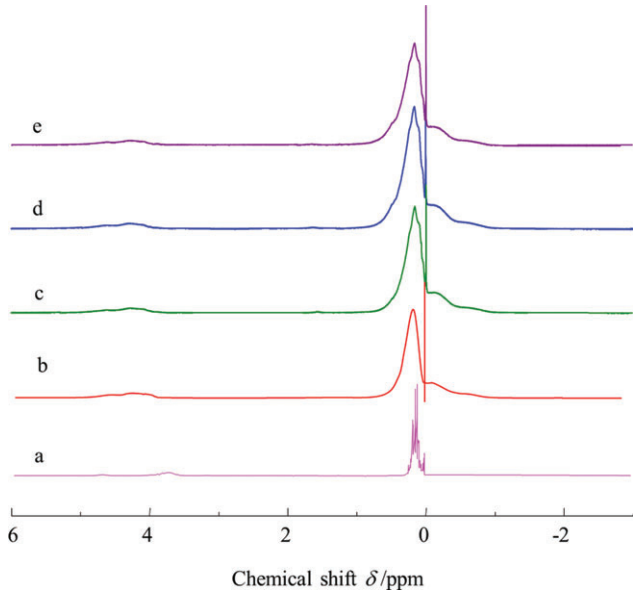

Figure 4. ^{1}H NMR spectra of PSCS and PMoCSs (a: PSCS, b: PCS, c: PMoCS-4 wt %, d: PMoCS-8 wt %, and e: PMoCS-10 wt %). [Color figure can be viewed in the online issue, which is available at wileyonlinelibrary.com].

Absorbency ratios between Si—H (2100 cm^{-1}) and Si—CH_3 (1252 cm^{-1}), A(Si—H)/A(Si—CH_3), are calculated based on Figure 2. The absorbency ratio in the function of the dosages of $MoCl_5$ is shown in Figure 3.

The absorbency ratio, as shown in Figure 3, decreases with the increasing dosages of $MoCl_5$. The reaction is therefore believed to involve HCl elimination between Si—H and Mo—Cl. Because each $MoCl_5$ molecule contains five Mo—Cl bonds, 1 moles of $MoCl_5$ can consume five moles of Si-H. Thus, $MoCl_5$ serving as a linkage reagent connects up to five PCS molecules. As could be noted in Table I, when the dosage of $MoCl_5$ is as low as 2 wt %, the molecular weight of the as-synthesized polymer is much higher than the Mo-free polymer synthesized at the same conditions.[39,40]

^{1}H NMR. The ^{1}H NMR spectra of PSCS, PCS, and PMoCSs are shown in Figure 4, where PMoCS-4 wt %, PMoCS-8 wt %, and PMoCS-10 wt % denotes PMoCS synthesized at 440°C for 10 h from PSCS and 4 wt %, 8 wt %, and 10 wt % $MoCl_5$, respectively.

Table II. Chemical Resonances and Integration Ratios of PSCS, PCS, and PMoCSs

Sample	Resonance (δ, ppm) Si—H	Molar ratio C—H	Si—H/C—H
PSCS	3.6-4.0	−0.2-0.3	0.132
PCS	3.8-5.4	−1.0-1.0	0.103
PMoCS-4 wt %	3.8-5.4	−1.0-1.0	0.092
PMoCS-8 wt %	3.7-5.4	−1.0-1.0	0.089
PMoCS-10 wt %	3.8-5.4	−1.0-1.0	0.085

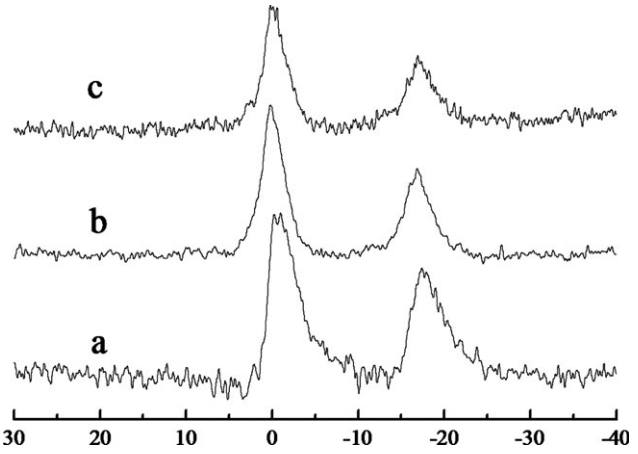

Figure 5. ^{29}Si NMR spectra PMoCSs (a: PMoCS-4 wt %, b: PMoCS-8 wt %, and c: PMoCS-10 wt %).

In Figure 4(a), the peaks centered at δ 3.8 ppm are assigned to the resonance of H in the Si—H bond in PSCS. From Figure 4(b) to (e), there are no obvious spectral differences among PCS, PMoCS-4 wt %, PMoCS-8 wt %, and PMoCS-10 wt %. The broad peak around δ 0 ppm corresponds to the resonance of H in the C—H bond, which is considered the overlap of three peaks at δ 0.4, −0.1, and −0.6 ppm. The peaks are attributed to the resonances of H in Si—CH_3, Si—CH_2, and Si—CH, respectively. The peak at δ 3.8–5.4 ppm corresponds to the resonance of H in the Si—H group in PMoCSs. All the peaks are consistent with those of PCS reported in the literature.[7,8,31,36–38] Based on the ^{1}H NMR results, the H molar ratios in Si—H and C—H are calculated from the integral values of the peaks, and the ratios are summarized in Table II.

As shown in Table II, the molar ratio between Si—H and C—H decreases with an increase in the dosages of $MoCl_5$, further confirming the HCl elimination between Si—H and Mo—Cl. The results are also consistent with the infrared data.

^{29}Si NMR. The ^{29}Si NMR spectra of PMoCSs are shown in Figure 5. All chemical shifts are referenced to tetramethylsilane as the internal standard. In Figure 5, the peak around δ −0.75 ppm is assigned to the resonance of Si in the SiC_4 unit, while

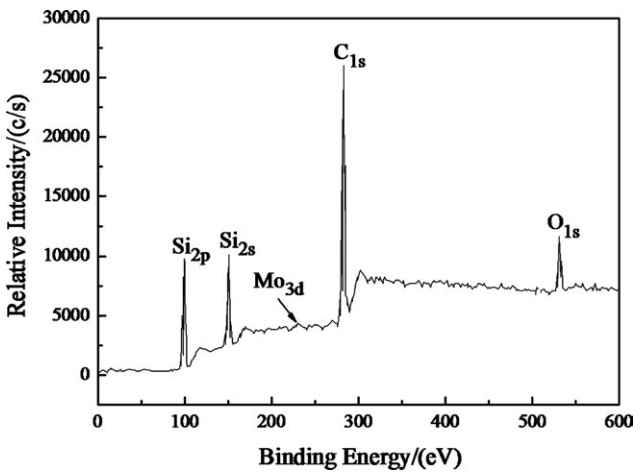

Figure 6. XPS spectrum of PMoCS-8 wt %.

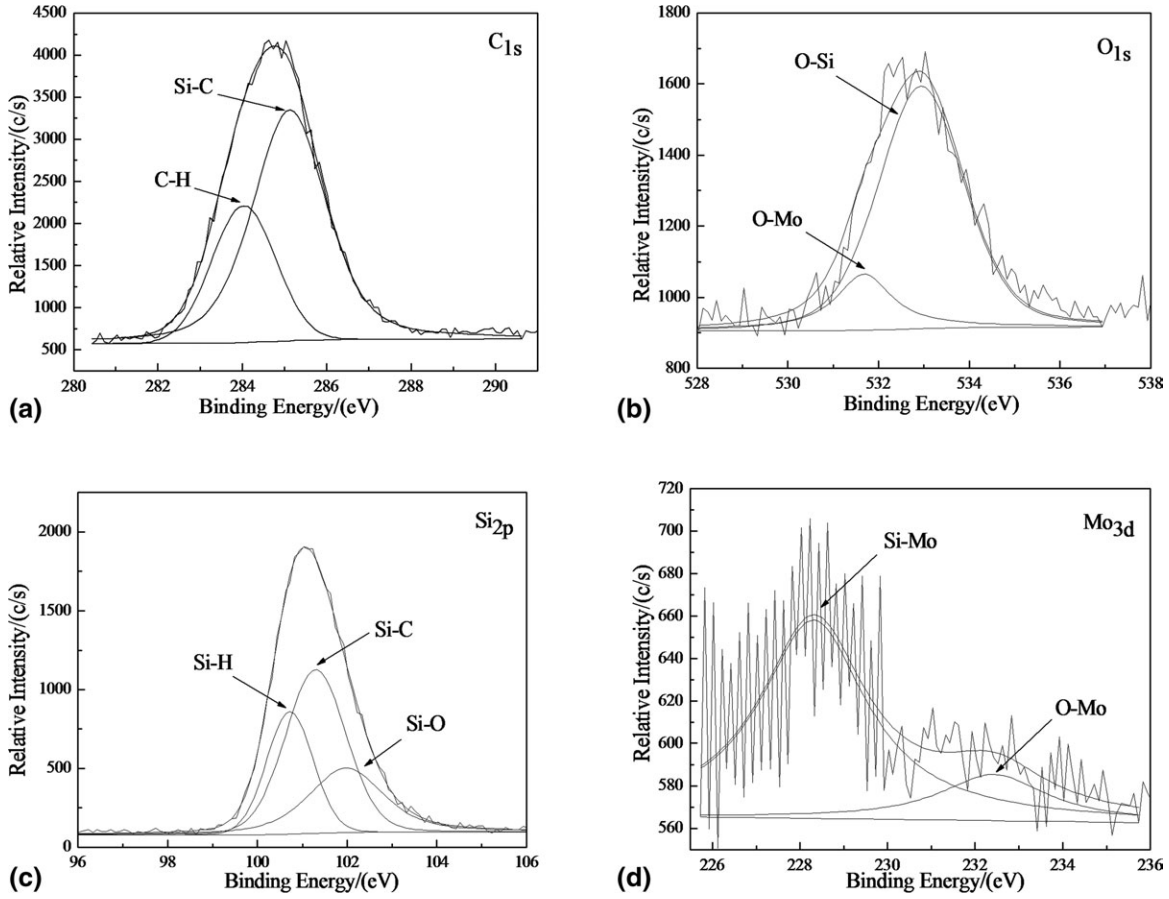

Figure 7. XPS spectra of Si_{2p}, C_{1s}, O_{1s}, and Mo_{3d}.

the peak at δ −17.5 ppm is the resonance of Si in the SiC_3H unit. The presence of only these two peaks suggests that Si exists mainly as SiC_4 and SiC_3H.[7,8,31,36–38] Again, Mo-Si bonds are not identified.

The ratio between SiC_3H and SiC_4 represents the degree of linearity of the polymer. Based on the peak integrals, the ratios between SiC_3H and SiC_4 in PMoCS-4 wt%, PMoCS-8 wt%, and PMoCS-10 wt % are about 0.855, 0.763, and 0.752, respectively, indicating that the SiC_3H units in these polymers are 46.08%, 43.29%, and 42.92%, respectively.[7,8,31,36–38] The SiC_4 units in them are, therefore, 53.92%, 56.71%, and 57.08%, respectively. Such results suggest a much lower degree of linearity than that of PCS.

XPS. The chemical environment in PMoCS-8 wt % was investigated with XPS. The XPS spectrum of is shown in Figure 6. The XPS spectrum of PMoCS-8 wt % features major peaks of Si_{2p} (101.9 eV), Si_{2s} (153 eV), C_{1s} (285.5 eV), O_{1s} (533.3 eV), and a peak for Mo_{3d} (228.5 eV).[7,8,31,36–42] The experimental and deconvoluted peaks attributed to Si_{2p}, C_{1s}, O_{1s}, and Mo_{3d} environments are revealed in Figure 7.

The XPS peaks of C_{1s} are composed of C—H (284.02 eV) and C—Si (285.11 eV), while the O_{1s} XPS peak consists of O—Mo (531.86 eV) and O—Si (533.49 eV).[7,8,31,36–42] The Si_{2p} peaks could be assigned to Si-H (100.72 eV), Si-C (101.29 eV), and Si-O (101.98 eV). In the Mo_{3d} spectrum, Si—Mo (228.31 eV) and O—Mo (232.43 eV) are observed. According to the peaks and their areas, Mo is found to exist mainly as Si-Mo bonds with a small part as Si—O—Mo bonds.[7,8,31,36–42] A relatively low oxygen content is also found in the polymer, where oxygen is thought to be introduced through the moisture in argon or the partial hydrolysis of $MoCl_5$.

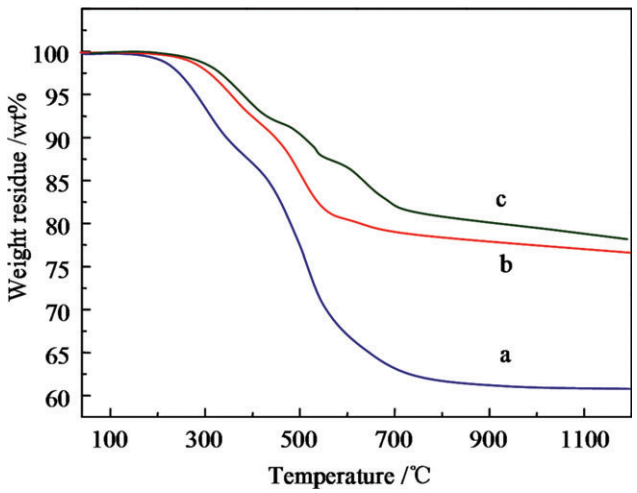

Figure 8. TGA curves of PCS (a), PMoCS-8 wt % (b), and PMoCS-10 wt % (c) recorded in a nitrogen flow at 10°C min^{-1}. [Color figure can be viewed in the online issue, which is available at wileyonlinelibrary.com.]

Table III. Elemental Compositions of PMoCS-8 wt %-Derived Ceramics and PCS

	Elemental compositions (wt %)					
	Si	C	O	Mo	H	Experimental formula
PMoCS-8 wt %	44.34	39.36	0.86	NA[c]	NA	$SiC_{2.073}H_mO_{0.034}Mo_n$
SiC(Mo)[a]	53.02	34.29	3.78	NA	NA	$SiC_{1.51}H_pO_{0.12}Mo_q$
SiC[b]	60.47	37.27	2.09	-	0.17 [d]	$SiC_{1.43}H_{0.079}O_{0.06}$

[a]PMoCS-8 wt %-derived ceramics, pyrolyzed at 1200°C in N_2 for 1 h, [b]PCS-derived ceramics, pyrolyzed at 1200°C in N_2 for 1 h, [c]Not available, [d]Calculated.

The reaction mechanism is thus proposed to consist of HCl elimination and, subseuqnently, the Kumada rearrangement. First, HCl elimination between Si—H and Mo—Cl occurrs at room temperature as shown in eq. (1), therefore forming a Si—Mo bond. The Si—O—Mo bond is produced by HCl elimination between Si—OH and Mo—Cl, as suggested in eq. (2).

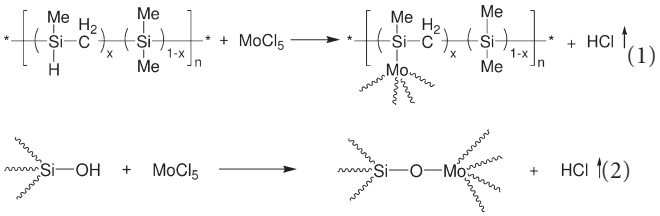

Second, the Kumada rearrangement proceeds when the temperature is raised above 360°C, as depicted in eq. (3).

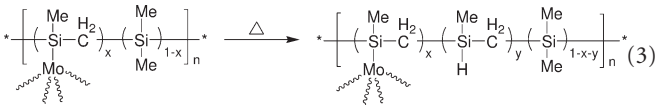

Polymer-to-Ceramic Conversion. The TGA curves of PMoCS-8 wt % and PMoCS-10 wt % are recorded in flowing nitrogen at 10°C min^{-1} as shown in Figure 8. For better comparison, a Mo-free polymer, PCS synthesized at 440°C for 10 h with a melting point of about 132°C, is also plotted in the figure.

As shown in Figure 8, the weight loss of PCS begins at about 200°C and is almost completed at around 700°C with a ceramic yield of 61.2%. The decomposition of PMoCS-8 wt % and PMoCS-10 wt % takes place at the temperature range from about 280 to 700°C, giving SiC(Mo) ceramics with ceramic yields of 77.1% and 78.5 %, respectively. The relatively high ceramic yields of PMoCSs are clearly related to the formation of the Si—Mo bridged bonds between the PCS chains that increase the linkage and therefore decrease the weight loss.

The elemental composition of the PMoCS-8 wt %-derived ceramics is measured, together with Mo-free polymer PCS for better comparison. The results are summarized in Table III.

The influence of the dosage of $MoCl_5$ on the phases of derived ceramics, pyrolyzed at 1200°C in N_2 for 1 h, is studied with XRD as shown in Figure 9. Broad peaks shown in Figure 9 at 36, 60, and 72° can be attributed to the (111), (220), and (311) diffraction lines of β-SiC crystals, respectively. Peaks at 41.87, 43.57, and 68.06°, on the other hand, can be attributed to the diffraction lines of β-$MoSi_2$ crystals. [34,35] With an increase in the dosage of $MoCl_5$, the content of β-$MoSi_2$ in the obtained ceramics increases. The grain size of β-SiC can be calculated according to the Scherrer equation, as eq. (4).

$$D = \frac{0.89 \cdot \lambda}{\beta \cdot \cos\theta} \tag{4}$$

where λ is 0.15406 nm, b is the half-height width of the diffraction peak (111), and θ is the angle in radians of the corresponding diffraction peak (111). The grain sizes of β-SiC in the derived ceramics from different PMoCS are shown in Table IV, together with the derived ceramics from Mo-free polymer PCS for better comparison.

The results show that, the grain size of β-SiC decreases while Mo is included. Mo, therefore, also plays a role as a grain

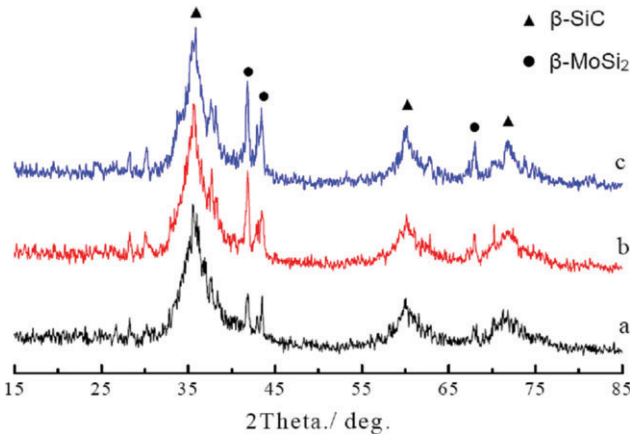

Figure 9. XRD patterns of PMoCS-derived ceramics pyrolyzed at 1200°C in N_2 for 1 h. PMoCS-6 wt %-derived ceramics (a), PMoCS-8 wt % derived ceramics (b), and PMoCS-10 wt %-derived ceramics (c). [Color figure can be viewed in the online issue, which is available at wileyonlinelibrary.com.]

Table IV. Grain Size of β-SiC in the Derived Ceramics Pyrolyzed at 1200°C in N_2 for 1 h

Precursor	Dosage of $MoCl_5$ (wt %)	Grain size of β-SiC (nm)
PCS	0	2.8
PMoCS-6 wt %	6	2.3
PMoCS-8 wt %	8	2.2
PMoCS-10 wt %	10	2.2

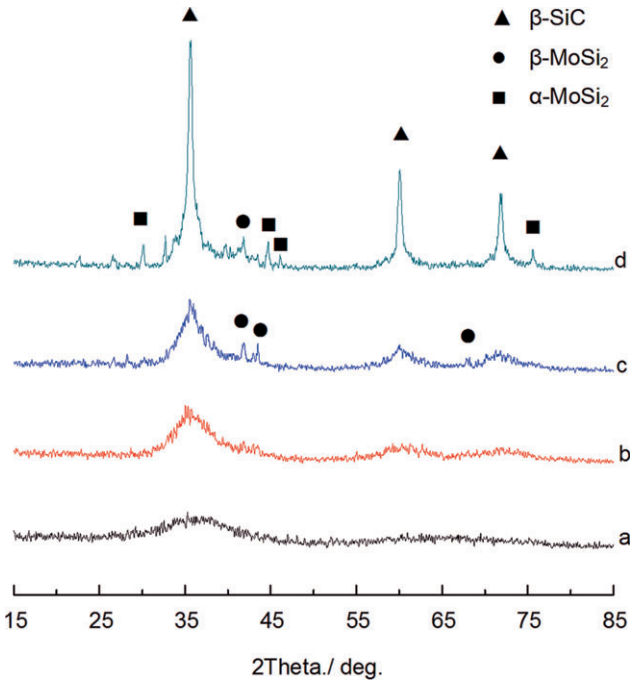

Figure 10. XRD patterns of PMoCS-8 wt %-derived ceramics pyrolyzed at 800 (a), 1000 (b), 1200 (c), and 1600°C (d) in N_2 for 1 h. [Color figure can be viewed in the online issue, which is available at wileyonlinelibrary.com].

growth inhibitor. It indicates that, the derived SiC(Mo) ceramics may exhibit good high-temperature resistance and excellent oxidation resistance. This study is now under investigation.

The XRD patterns of PMoCS-8 wt %-derived ceramics isolated at different temperatures from 800 to 1600°C for an isothermal duration of 1 h are presented in Figure 10.

Phase identification in Figure 10 is achieved through locating the characteristic diffraction peaks of the respective phases in the XRD patterns. Ceramics pyrolyzed in the range of 800–1000°C are all amorphous. In the pattern of Figure 10(c), peaks at 41.87°, 43.57°, and 68.06° can be attributed to the diffraction lines of β-$MoSi_2$ crystals, [34,35] while in the pattern of Figure 10(d), peaks at 30.08°, 44.69°, 46.28°, and 75.60° can be assigned to the (101), (103), (004), and (213) diffraction lines of α-$MoSi_2$ crystals, respectively.[34,35] These findings suggest the conversion from β-$MoSi_2$ to α-$MoSi_2$ is nearly completed at about 1600°C.

Table V. Melt-Spinning Conditions of PMoCSs

Polymers	PMoCS-2 wt %	PMoCS-4 wt %	PMoCS-8 wt %
$\overline{Mn}$[a]	1656	1801	2016
$\overline{Mw}$[b]	7081	10093	12930
Melten point (°C)	150	169	185
Spinning Temperature (°C)	270	270	320
Pressure (MPa)	0.6	0.6	0.7
Take-up speed ($m \cdot min^{-1}$)	300	350	400
Diameter of green fiber (μm)	13.4	13.2	12.2

[a]Number average molecular weight according to the GPC results, [b]Weight average molecular weight according to the GPC results.

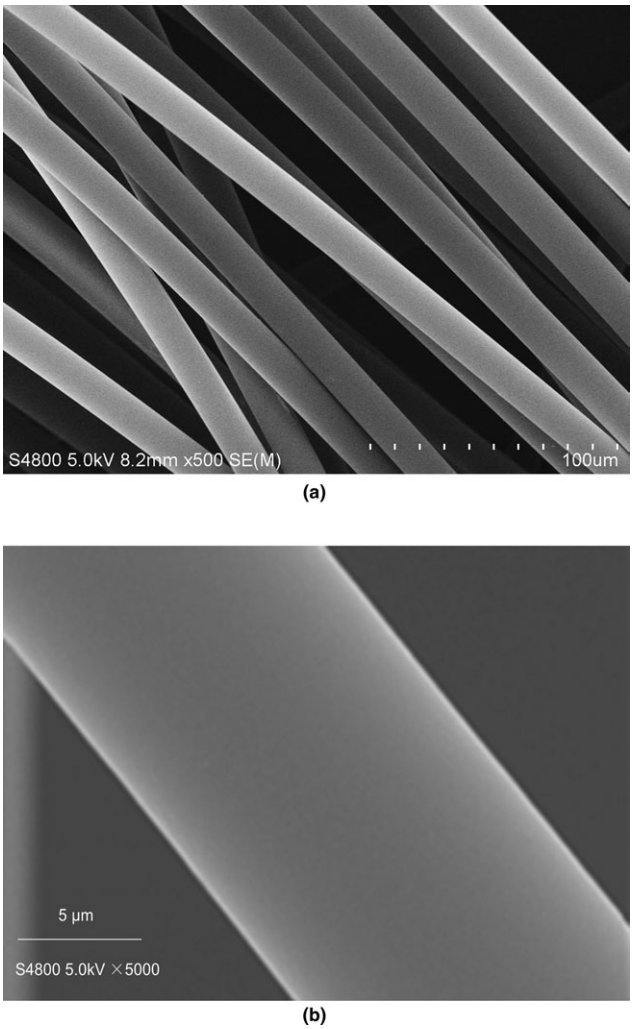

Figure 11. SEM images of the as-spun green fibers from PMoCS-8 wt % × 500 (a) and × 5000 (b).

Preliminary Research on the Melt Spinnability of PMoCS

PMoCSs prove to be a tractable polymers with a wide range of viscoelastic properties that render them potential candidates for shaping processes such as melt-spinning were obtained. The spinnability of PMoCS is tested using a labscale melt-spinning apparatus with a single-capillary spinneret of 200 nm in diameter. PMoCS-2 wt %, PMoCS-4 wt %, and PMoCS-8 wt % show excellent spinnability under the conditions shown in Table V. The PMoCS is readily melt spinnable into flexible and uniform fine-diameter green fibers.

For example, the scanning electron microscopy (SEM) images of the as-spun green fibers from PMoCS-8 wt % are shown in Figure 11. It is shown that the green fibers are regular in diameter (13.4–12.2 μm), smooth and without surface defects. This study is now under investigation.

CONCLUSIONS

PMoCSs have been synthesized through HCl elimination between PSCS and $MoCl_5$ as raw materials, and followed by the Kumada rearrangements. The reaction is a temperature-dependent process, where the reaction temperature requires to be less than 450°C.

$MoCl_5$ serving as a linkage reagent connects up to five PCS molecules. The molecular weight of the as-synthesized polymer increases rapidly with the increasing dosages of $MoCl_5$. The as-synthesized polymer is air- and moisture-stable, fusible, soluble in organic solvents, and therefore suitable for spinning fibers. The structures of PMoCS are investigated with multiple spectroscopic techniques. Mo exists mainly as Si—Mo bond based on the XPS results. Mo-containing PCS shows higher ceramic yields than Mo-free PCS. The ceramic yield of PMoCS-10 wt % is measured approximately at 78.5% from TGA at 1200°C in a N_2 flow. After pyrolyzed, PMoCS is converted to $MoSi_2$-containing β-SiC ceramics, and β-$MoSi_2$ crystals are formed at 1400°C. The conversion from β-$MoSi_2$ to α-$MoSi_2$ is almost completed at 1600°C. Mo atoms are found to play a role as a grain growth inhibitor. The grain size of β-SiC decreases when Mo is increased. PMoCS is melt spinnable into flexible and uniform green fibers with the diameters about 13.4 μm to 12.2 μm.

ACKNOWLEDGMENTS

The financial support by the National Science Foundation of China (Project No. 90916002) and State Key Laboratory (Project No. 9140C8201020901) is gratefully acknowledged.

REFERENCES

1. Riedel, R.; Mera, G.; Hauser, R.; Klonczynski, A. *J. Ceram. Soc. Jpn.* **2006,** *114*, 425.
2. Miele, P.; Bernard, S.; Cornu, D.; Toury, B. *Soft Mater.* **2006,** *4*, 249.
3. Colombo, P.; Mera, G.; Riedel, R.; Sorarù, G. D. *J. Am. Ceram. Soc.* **2010,** *93*, 1805.
4. Bunsell, A. R.; Plant, A. *J. Mater. Sci.* **2006,** *41*, 823.
5. Okamura, K.; Shimoo, T.; Suzuya, K.; Suzuki, K. *J. Ceram. Soc. Jpn.* **2006,** *114*, 445.
6. Zhao, D. F.; Wang, H. Z.; Li, X. D. *J. Inorg. Mater.* **2009,** *6*, 1097.
7. Yajima, S.; Hayashi, J.; Omori, M.; Okamura, K. *Nature* **1976,** *261*, 683.
8. Birot, M.; Pillot, J. P.; Dunogues, J. *Chem. Rev.* **1995,** *95*, 1443.
9. Bernard, S.; Weinmann, M.; Cornu, D.; Miele, P.; Aldinger, F. *J. Eur. Ceram. Soc.* **2005,** *25*, 251.
10. Bernard, S.; Weinmann, M.; Gerstel, P.; Miele, P.; Aldinger, F. *J. Mater. Chem.* **2005,** *5*, 289.
11. Kroke, E.; Li, Y. L.; Konetschny, C.; Lecomte, E.; Fasel, C.; Riedel, R. *Mater. Sci. Eng.* **2000,** *26*, 97.
12. Yan, X. B.; Gottardo, L.; Bernard, S.; Dibandjo, P.; Brioude, A.; Moutaabbid, H.; Miele, P. *Chem. Mater.* **2008,** *20*, 6325.
13. Yuan, X. Y.; Lü, J. W.; Yan, X. B.; Hua, L. T.; Xue, Q. J. *Micro. Meso. Mater.* **2011,** *142*, 754.
14. Majoulet, O.; Alauzun, J. G.; Gottardo, L.; Gervais, C.; Schuster, M. E.; Bernard, S.; Miele, P. *Micro. Meso. Mater.* **2011,** *140*, 40.
15. Günthner, M.; Kraus, T.; Dierdorf, A.; Decker, D.; Krenkel, W.; Motz, G. *J. Euro. Ceram. Soc.* **2009,** *29*, 2061.
16. Hauser, R.; Borchard, S. N.; Ralf, R. *J. Ceram. Soc. Jpn.* **2006,** *114*, 524.
17. Li, J.; Bernard, S.; Salles, V.; Gervais, C.; Miele, P. *Chem. Mater.* **2010,** *22*, 2010.
18. Yajima, S.; Hasegawa, Y.; Okamura, K.; Matsuzawa, T. *Nature* **1978,** *273*, 525.
19. Ishikawa, T.; Kohtoku, Y.; Kumagawa, K.; Yamamura, T.; Nagasawa, T. *Nature* **1998,** *391*, 773.
20. Xue, J. G.; Wang, Y. D.; Song, Y. C. *J. Inorg. Mater.* **2007,** *22*, 681.
21. Tang, Y.; Wang, J.; Li, X. D.; Li, W. H.; Wang, H. *J. Inorg. Mater.* **2008,** *23*, 525.
22. Yang, D. X.; Song, Y. C. *Eng. Mater.* **2008,** *368–372*, 827.
23. Zhao, D. F.; Li, X. D.; Wang, H.; Zheng, C. M.; Wang, H. Z. *Rare Metal. Mater. Eng.* **2008,** *S1*, 729.
24. Tang, Y.; Wang, J.; Li, X.; Xie, Z.; Wang, H.; Li, W.; Wang, X. *Chem. Eur. J.* **2010,** *16*, 6458.
25. Tang, Y.; Wang, J.; Li, X.; Xie, Z.; Wang, H.; Wang, Y. *Inorg. Chem. Commun.* **2009,** *12*, 602.
26. Ishikawa, T.; Kohtoku, Y.; Kumagawa, K. *J. Mater. Sci.* **1998,** *33*, 161.
27. Ichikawa, H. *J. Ceram. Soc. Jpn.* **2006,** *114*, 454.
28. Narisawa, M.; Tanno, H.; Ikeda, M.; Iseki, T.; Mabuchi, H.; Okamura, K.; Oka, K.; Dohmaru, T. Kim, D.P. *J. Ceram. Soc. Jpn.* **2006,** *114*, 558.
29. Liu, L.; Li, X. D.; Xing, X.; Zhou, C. C.; Hu, H. F. *J. Organometall. Chem.* **2008,** *693*, 917.
30. Lee, Y. J.; Lee, J. H.; Kim, S. R.; Kwon, W. T.; Oh, H.; Klepeis, J. P.; Teat, S. J.; Kim, Y. H. *J. Mater. Sci.* **2010,** *45*, 1025.
31. Xie, Z. F.; Cao, S. W.; Wang, J.; Yan, X. B.; Bernard, S.; Miele, P. *Mater. Sci. Eng. Part A: Structur. Mater. Propert. Microstructure Process.* **2010,** *527*, 7086.
32. Hasagawa, Y. *J. Ceram. Soc. Jpn.* **2006,** *114*, 480.
33. Ralf, R.; Kienzle, A.; Dressler, W. *Nature* **1996,** *382*, 796.
34. Meier, S.; Heinrich, J. G. *J. Eur. Ceram. Soc.* **2002,** *22*, 2357.
35. Wang, H.; Li, X.; Kim, D. *Appl. Organometal. Chem.* **2005,** *19*, 742.
36. Hasegawa, Y.; Okamura, K. *J. Mater. Sci.* **1986,** *21*, 321.
37. Cheng, X. Z.; Xie, Z. F.; Song, Y. C.; Xiao, J. Y. *J. Inorg. Organometal. Polym. Mater.* **2005,** *15*, 253.
38. Cheng, X. Z.; Xie, Z. F.; Song, Y. C.; Xiao, J. Y.; Wang, Y. D. *Int. J. Polym. Anal. Charact.,* **2006,** *11*, 287.
39. Yajima, S.; Hasegawa, Y.; Hayashi, J. *J. Mater. Sci.* **1978,** *13*, 2569.
40. Cheng, X. Z.; Xie, Z. F.; Song, Y. C.; Xiao, J. Y.; Wang, Y. D. *J. Appl. Polym. Sci.* **2006,** *99*, 1188.
41. Kim, D. *Mater. Res. Bull.* **2001,** *36*, 2497.
42. Hirayama, M. K. N.; Caseri, W. R.; Suter, U. W. *Appl. Surf. Sci.* **1999,** *143*, 256.